

# A Generalized Estimating Equation Approach to Network Regression

Riddhi Pratim Ghosh<sup>1</sup>, Jukka-Pekka Onnela<sup>2</sup>, and Ian Barnett<sup>3</sup>

<sup>1</sup>Department of Mathematics and Statistics, Bowling Green State University

<sup>2</sup>Department of Biostatistics, Harvard University

<sup>3</sup>Department of Biostatistics, University of Pennsylvania

## Abstract

Regression models applied to network data where node attributes are the dependent variables poses a methodological challenge. As has been well studied, naive regression neither properly accounts for community structure, nor does it account for the dependent variable acting as both model outcome and covariate. To address this methodological gap, we propose a network regression model motivated by the important observation that controlling for community structure can, when a network is modular, significantly account for meaningful correlation between observations induced by network connections. We propose a generalized estimating equation (GEE) approach to learn model parameters based on clusters defined through any single-membership community detection algorithm applied to the observed network. We provide a necessary condition on the network size and edge formation probabilities to establish the asymptotic normality of the model parameters under the assumption that the graph structure is a stochastic block model. We evaluate the performance of our approach through simulations and apply it to estimate the joint impact of baseline covariates

and network effects on COVID-19 incidence rate among countries connected by a network of commercial airline traffic. We find that during the beginning of the pandemic the network effect has some influence, the percentage of urban population has more influence on the incidence rate compared to the network effect after the travel ban was in effect.

*Keywords:* network regression; transportation networks; generalized estimating equations; COVID-19

# 1 Introduction

Network data provide quantitative information to study and unveil the pattern of interactions among various objects from individuals to countries. The inferential task in scientific applications requires learning about the influence that an individual has on others, which is further complicated as the individuals are often nested in communities. Two important methodological challenges of network regression are (1) accounting for correlation induced by network structure, and (2) allowing for node attributes to appear in the data both as outcome as well as covariates in the design matrix. For example, network regression was applied in the study of the nature and extent of the person-to-person spread of obesity, Christakis & Fowler (2007) found that obesity appears to spread through social ties, a phenomenon that may in part be explained by the notion of homophily – that birds of a feather flock together (Shrum et al., 1988; Igarashi et al., 2005; Tifferet, 2019). Sensitivity analyses suggest that contagion effects for obesity and smoking cessation are reasonably robust to possible latent homophily or environmental confounding; those for happiness and loneliness are somewhat less so (VanderWeele, 2011). To further investigate the causal relationship, Shalizi & Thomas (2011) provided three factors underlying such interaction: homophily, or the formation of social ties due to matching individual traits; social contagion; the causal effect of an individual’s covariates on his or her measurable responses; and an individual’s response. This has led to the development of two types of models: (1) community detection models that aim to find distinct communities or clusters of similar individuals (Holland et al., 1983; Newman, 2018), and (2) a more general framework of network regression that can model such phenomenon using a direct link between observed individual attributes or covariates and the network interactions (Holland & Leinhardt, 1981; P. D. Hoff et al., 2002; P. Hoff, 2021). Some approaches that aim at merging the above two models exploit distributional assumptions to incorporate covariate information in detecting communities in the network (Binkiewicz et al., 2017; Mu et al., 2022). These examples highlight the need for regression techniques that are robust to non-trivial network structure because in all these

studies community labels are known which makes the evaluation of covariate effects easy. However, in a more realistic situation, community labels are unknown (unobserved) with differences in covariates existing through the unobserved communities making the inference challenging.

In this article, we aim to develop a network regression model motivated by the important observation that the differences between the communities in a network can be attributed to the differences in the influences of covariates responsible for an edge formation. Our model is based on a flexible network effect assumption, and it allows us to perform tests for the model parameters in addition to the estimation. Aside from detecting communities solely based on degree, the degree corrected stochastic block model was one of the first model that allows within community heterogeneity (Qin & Rohe, 2013). There has been a surge of interests among psychologists and social scientists to study such behavior- Aukett et al. (1988) shows that gender difference plays an important role in friendship patterns: women shows a preference for a few, closer, intimate same-sex friendships based on sharing emotions whereas men build up friendship based on the activities they do together. Staber (1993) studies how women and men form entrepreneurial relationships, concluding that women's networks are wider with more strangers and higher proportion of cross-sex ties. In each of these network regression examples, community labels are known which alleviates the inferential task of finding the effects of covariates and learning community structures. However, in many other scenarios, community labels are unknown which makes the inferential task more challenging. For example, here we will consider the network regression problem of seeing the impact of air travel network flow between countries on COVID-19 incidence rates, where network structure is unknown and must be estimated. The current literature lacks powerful methods that can address this important issue. Our focus is to bridge this gap by leveraging covariate-assisted information to propose an effective tool which also accounts for the network modeling through adjacency matrix.

Generalized estimating equations (GEE) (Liang & Zeger, 1986; Zeger, 1986) provide a

popular approach that is often used to analyze longitudinal and other types of correlated data (Burton et al., 1998; Diggle et al., 2002; Mandel et al., 2021) We propose first performing community detection in order to estimate community membership before then using a GEE regression model to account for the resulting estimated community structure. This approach is general and agnostic to the community detection algorithm used so long as each node can belong to at most one community. Given that network regression needs to account for correlation between attributes from nodes that are connected, a GEE allows for arbitrary correlation between nodes within the same community. Of note, this approach is best suited for highly modular networks so that the GEE assumption of independence between different communities is more accurate, though we explore its performance in less modular networks with more between-community mixing.

The rest of this article is organized as follows. In Section 2 we introduce our network regression model along with our GEE extension, and we describe the transportation network we use to model country-specific COVID-19 incidence rates. In Section 3 we present the theoretical results followed by extensive simulation results and real data analysis. Finally, Section 4 concludes the article with a discussion.

## 2 Methods

In this section, we introduce our network regression model and describe the air travel networks for each month of the first quarter of 2020 (the beginning of the COVID-19 pandemic) with country-specific information such as COVID-19 incidence rate, GDP, and population size. Next, we present a generalized estimating equation (GEE) approach to network regression that accounts for network-induced correlation between observations.

## 2.1 Model and notation

We consider a directed network of  $n$  nodes and an  $n \times n$  adjacency matrix  $\mathbf{A} = (a_{ij})$  with 0's on the diagonal (i.e. no self-loops). We denote the feature variable of the  $i$ th node by  $y_i$ , the  $l$ -dimensional vector of covariates by  $\boldsymbol{\alpha}$ , and the corresponding design matrix by  $\mathbf{x}_i$ . Denoting the coefficient of interest by  $\beta$ , the network regression model for node attribute  $y_i$  we consider:

$$y_i = \boldsymbol{\alpha}^\top \mathbf{x}_i + \beta \cdot \sum_{j \neq i} A_{ji} y_j / (n - 1) + \epsilon_i, \quad (1)$$

where  $\epsilon_i \stackrel{iid}{\sim} N(0, \sigma^2)$  and  $\boldsymbol{\alpha} \in \mathbb{R}^l$ . One can note that the above model is reminiscent of the first-order autoregressive spatial model of Kelejian & Prucha (1998) which frequently contains a spatial lag of the dependent variable as a covariate that is spatially autoregressive.

Using vector and matrix notation, the above model can also be written as

$$\mathbf{y} = \mathbf{X}^\top \boldsymbol{\alpha} + \beta \cdot \mathbf{A}\mathbf{y} / (n - 1) + \boldsymbol{\epsilon},$$

where  $\mathbf{y}$  is the concatenation of the  $y_i$ s in a vector of length  $n$ , and  $\mathbf{X} = [\mathbf{x}_1 : \mathbf{x}_2 : \dots : \mathbf{x}_n]$ , is the matrix of covariates. Note, model (1) can be trivially adapted to generalized linear models with non-linear link functions and non-Gaussian data in the scope of GEE models.

## 2.2 Data description

With 622 million confirmed cases and 6.5 million deaths globally as of October 01, 2022, the COVID-19 pandemic has had a tremendous impact on the world, shrinking the global economy by 5.2%, the largest recession in the history post World War II (Bank, 2020). The travel bans in places worldwide have severely affected the tourism industry, with estimated losses of 900 billion to 1.2 trillion USD and tourism down 58%-78% (Le et al., 2022). The

airline industry has also suffered heavily, with 43 airlines declaring bankruptcy and 193 of 740 European airlines at risk of closing. Here we focus on the start of the pandemic covering the transition to travel bans across the world to study the relative effectiveness of travel bans for controlling and contributing to COVID-19 incidence rates.

We use pandemic data from the Johns Hopkins University coronavirus data repository through April 30, 2020, (COVID, 19). Flight data are from the Official Airline Guide (OAG) (Strohmeier et al., 2021). Because only data for January and February 2020 are available from OAG, we used the estimated flight data for other time periods using the OpenSky Network database (Schäfer et al., 2014; Strohmeier et al., 2021). This database tracks the number of flights from one country to another over time, which we use to estimate country-to-country flight data for other months. We include as covariates the GDP, total population, and percentage of the urban population for each country in our network. Constructing a network based on by the flight data and incorporating the above country-specific attributes such as GDP, population, etc. as covariates through  $\alpha$  in (1), we aim to estimate the effectiveness of travel bans through  $\beta$  in model (1).

### 2.3 Generalized estimation equation (GEE) approach

Our network contains  $K$  communities where community  $k$  is defined by

$$E_k = \{i : g_i = k\},$$

where index  $g_i$  represents the community membership of node  $i$ ,  $|E_k| = n_k$  (number of nodes in community  $k$ ) and  $\sum n_k = n$ . Let  $\mathbf{y}_k$  and  $\boldsymbol{\epsilon}_k$  denote the concatenated vectors of  $y_{ij}$ s and  $\epsilon_{ij}$ s respectively, and  $\mathbf{X}_k = [\mathbf{x}_1, \mathbf{x}_2, \dots, \mathbf{x}_{n_k}]$  denote the  $l \times n_k$  sub-matrix of covariates corresponding to cluster  $k$ .

To fit our network regression model in the GEE framework, we use communities as clusters and use the following equation to model the node attributes of members of the  $k$ th

cluster:

$$\mathbf{y}_k = \mathbf{X}_k^\top \boldsymbol{\alpha} + \beta \mathbf{Z}_k + \boldsymbol{\epsilon}_k, \quad (2)$$

where  $\mathbf{A}_k$  is the  $n_k \times n_k$  sub-matrix of  $\mathbf{A}$  pertaining to the cluster  $k$ , and  $\mathbf{Z}_k = \mathbf{A}_k \mathbf{y}_k / (n-1)$ .

The marginal mean  $\boldsymbol{\mu}_k$  of  $\mathbf{y}_k$  has the form:

$$\boldsymbol{\mu}_k = E(\mathbf{y}_k | \mathbf{X}_k) = (\mathbf{I}_{n_k} - \beta \mathbf{A}_k / (n-1))^{-1} \mathbf{X}_k^\top \boldsymbol{\alpha}, \quad k = 1, 2, \dots, K,$$

where  $\mathbf{I}_{n_k}$  is the identity matrix of order  $n_k$ .

Adopting a GEE approach (Liang & Zeger, 1986), the resulting estimating equation is given by

$$\sum_{k=1}^K \mathbf{D}_k^\top \mathbf{V}_k^{-1} (\mathbf{y}_k - \boldsymbol{\mu}_k) = \mathbf{0}, \quad k = 1, 2, \dots, K, \quad (3)$$

where  $\mathbf{D}_k = \frac{\partial \boldsymbol{\mu}_k}{\partial (\beta, \boldsymbol{\alpha})^\top}$  is of dimension  $n_k \times (l+1)$  and  $\mathbf{V}_k$  is the  $n_k \times n_k$  working covariance matrix of  $\mathbf{y}_k$ . The explicit form for  $\mathbf{D}_k$  is

$$\mathbf{D}_k = [- \underbrace{(\mathbf{I}_{n_k} - (\beta/(n-1)) \mathbf{A}_k)^{-1} \mathbf{A}_k (\mathbf{I}_{n_k} - (\beta/(n-1)) \mathbf{A}_k)^{-1} \mathbf{X}^\top \boldsymbol{\alpha}}_{n_k \times 1} : \underbrace{(\mathbf{I}_{n_k} - (\beta/(n-1)) \mathbf{A}_k)^{-1} \mathbf{X}_k^\top}_{n_k \times l}].$$

One can note that  $\mathbf{D}_k$  consists of two partitioned matrices where the first one corresponds to the network parameter  $\beta$  and the second one is due to the covariate  $\boldsymbol{\alpha}$ . We can solve for  $\hat{\boldsymbol{\alpha}}$  and  $\hat{\beta}$  in equation (3) through iterative reweighted least squares, and use the robust sandwich covariance estimator to perform inference on  $\boldsymbol{\alpha}$  and  $\beta$ .

## 3 Results

### 3.1 Theoretical results

In this section, we prove the asymptotic normality of the resulting GEE estimator for  $\beta$  and  $\alpha$  jointly. Towards this, we assume constant probabilities of edge formation between and within communities where we denote these quantities by  $p$  and  $q$  respectively as in a stochastic block model (Holland et al., 1983). Our proof of asymptotic normality hinges on Theorem 2 of Liang & Zeger (1986) which establishes the asymptotic normality of the regression parameter in the classical GEE approach under the assumption that the correlation parameter appropriately scaled by the number of communities is consistent. Our primary distinction from this approach is that we must account for probabilities of edge formation instead of correlation between observations. Therefore, we first establish the consistency of  $p$  and  $q$  following Proposition 1 of Chen et al. (2021) and subsequently show asymptotic normality of  $(\hat{\beta}, \hat{\alpha})$  from the estimating equation (3).

#### 3.1.1 Consistency of $\hat{p}$ and $\hat{q}$

**Proposition 3.1.** Consider a network generated from a stochastic block model of  $K$  communities of size  $m$  so that total number of nodes is  $n = Km$ . Assume that  $m^\gamma p \rightarrow p^*$  and  $m^\gamma q \rightarrow q^*$  as  $n \rightarrow \infty$ , where  $p^*$  and  $q^*$  are positive fixed constants, and  $\gamma \in [0, 2)$ , then  $m^{1+\gamma/2}(\hat{p} - p)$  and  $m^{1+\gamma/2}(\hat{q} - q)$  are both  $o_P(1)$ .

*Proof.* See the appendix in Section 5.1. □

Guided by the above proposition, we establish the asymptotic normality of the model parameters in the following theorem. The key difference with the classical formula is the inclusion of the community size in the covariance coming from the consistency of  $p$  and  $q$ .

### 3.1.2 Asymptotic normality of $\hat{\beta}$

**Theorem 3.2.** Under the conditions of Proposition 3.1  $K^{1/2}m^{1+\gamma/2}((\hat{\beta}, \hat{\alpha}) - (\beta, \alpha))^\top$  is asymptotically multivariate normal with zero mean and covariance given by

$$V = \lim_{K \rightarrow \infty} K m^{2+\gamma} \left( \sum_{k=1}^K \mathbf{D}_k^\top \mathbf{V}_k^{-1} \mathbf{D}_k \right)^{-1} \left( \sum_{k=1}^K \mathbf{D}_k^\top \mathbf{V}_k^{-1} \text{cov}(\mathbf{Y}_k) \mathbf{V}_k^{-1} \mathbf{D}_k \right) \left( \sum_{k=1}^K \mathbf{D}_k^\top \mathbf{V}_k^{-1} \mathbf{D}_k \right)^{-1}$$

*Proof.* See the appendix in Section 5.2. □

*Remark:* The variance formula involves the term  $m^{2+\gamma}$ , where  $m$  is the community size. If  $m$  is large, then the covariance will increase at a rate  $m^{2+\gamma}$ . This is reminiscent of the well-known fact that sandwich estimator  $\hat{V}$  of the covariance of  $(\beta, \alpha)^\top$  is not stable if  $m$  is large relative to  $K$ . In essence, if  $m$  grows at a similar rate to  $K$  the sandwich estimator becomes and unstable estimator of covariance. In practice this implies that the GEE approach works best when the network contains many smaller communities rather than only a few larger communities.

## 3.2 Simulations

We simulate a network of  $n$  nodes having balanced communities of size  $m = 10$  via a stochastic block model and vary  $n$  in  $\{200, 400\}$  with the number of communities ( $K$ ) being 20 and 40 for both values of  $n$ , respectively. Let  $p$  and  $q$  denote the within community and between community probabilities of an edge formation as in a stochastic block model. In each setting, we vary  $(p, q) \in \{(0.8, 0), (0.7, 0.1), (0.6, 0.2), (0.5, 0.3)\}$ .

### 3.2.1 Estimation of $\beta$ and $\alpha$

The choice of true model parameters and the corresponding data-generating process are detailed to span networks with varying degrees of modularity. We set  $\beta_0 = 0.5$  and  $\alpha_0 =$

$(1, 1, 1, 1, 0.5, 0.5, 0.5, -0.5, -0.5, 2)^\top$  ( $l = 10$  in equation (1)). We simulate the  $l \times n$  matrix  $\mathbf{X}$  by a multivariate normal distribution in the following manner. The  $j$ th column of  $\mathbf{X}$ , if it belongs to community  $k$  ( $k = 1, 2, \dots, K$ ), follows  $\text{MVN}((k/10)\mathbf{1}_l, 0.0001\mathbf{I}_l)$ , where  $\mathbf{1}_l$  and  $\mathbf{I}_l$  are the vector with 1s and identity matrix of dimension  $l$ , respectively. In each setting, the adjacency matrix  $\mathbf{A}$  of dimension  $n$  is simulated by the stochastic block model which has  $K$  communities of the aforementioned size such that within and between community edge probabilities are  $p$  and  $q$ , respectively. Finally, the response variable  $y_i$  is generated according to equation (1) with  $\sigma = 0.01$ .

To estimate  $\beta$  and  $\boldsymbol{\alpha}$ , we first perform a community detection on the directed graph obtained from the adjacency matrix  $\mathbf{A}$  as in Rosvall & Bergstrom (2007). Next, with the resulting communities we fit a GEE using the *geepack* R package (Halekoh et al., 2006) and report the estimates of bias and variance by taking the average of over  $B = 1000$  replications.

The squared bias and variance of the estimated  $\beta$  increase as the networks become less modular (i.e.  $q$  increases) for both our GEE approach as well as naive least squares (see Figure 1). The naive least squares method does not assume any community structure and reports the parameter estimates from assuming independence between observations using equation (1) directly.

From Figure 1 we see that less modular networks are more difficult to fit in general based on the increase in bias for both methods. Despite this our GEE approach uniformly is less biased than naive least squares, which demonstrates that controlling for correlation within communities is effectively done by GEE. This also exposes the weakness of our GEE approach: if the network is not modular with high degrees of mixing between communities (i.e. large  $q$ ) the GEE framework cannot accommodate this due its assumption of independence between communities. However, even when  $q$  is large we still observe that GEE somewhat mitigates the impact of correlation induced by the network at least partially, which explains why its bias is smaller than that of naive least squares. Essentially, even when the network structure suggests the GEE assumptions are incorrect, one is still generally better

off partially accounting for network structure using our GEE approach rather than ignore community structure altogether.

The smaller standard errors demonstrated by least squares in Figure 1 reflect the inaccuracy of the method. By ignoring community structure and assuming independence between observations in network regression settings, we expect to see anti-conservative hypothesis tests, too-narrow confidence intervals, and general overconfidence. This overconfidence is reflected in the too-small standard errors for naive least squares as well as in the anti-conservative Type I errors we demonstrate next.

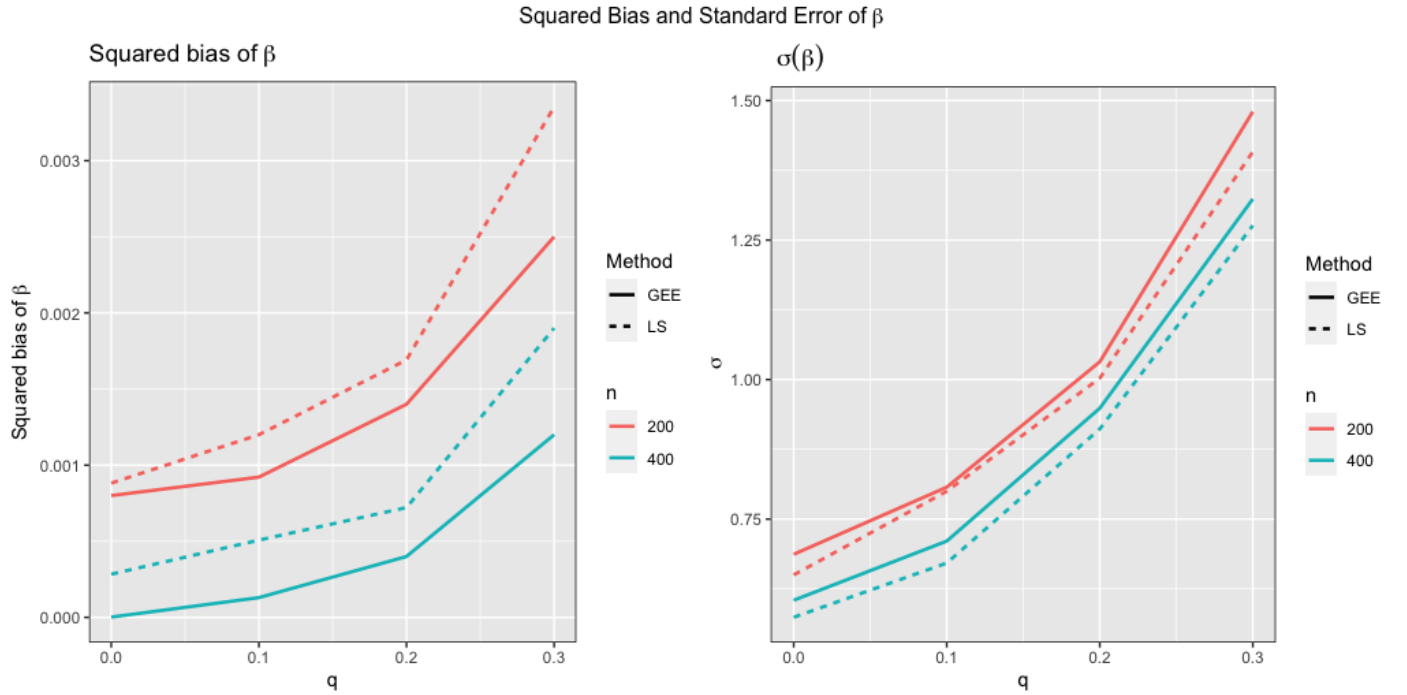


Figure 1: **Bias squared and standard error of estimates of  $\beta$  with varying degrees of network modularity.** In order to estimate  $\beta$   $B = 1000$  replications were performed for  $n = 200, 400$  with the average degree 7 and 16 respectively. The values of  $(p, q)$  are varied over  $\{(0.8, 0), (0.7, 0.1), (0.6, 0.2), (0.5, 0.3)\}$ .

### 3.2.2 Hypothesis testing of $\beta$

We consider an approach to testing the hypothesis of  $H_0 : \beta = 0$  against the alternative  $H_A : \beta \neq 0$ . We perform a simulation study to obtain Type I error in a variety of network

structures. We consider two working correlation structures for our GEE model: independence and exchangeable. First, we simulate our data as in Section 3.2 with  $\beta = 0$ . We obtain an empirical null distribution by replicating this procedure  $B = 1000$  times to obtain  $\hat{\beta}^{(1)}, \hat{\beta}^{(2)}, \dots, \hat{\beta}^{(B)}$ . We estimate the P-value by  $\sum_{b=1}^B I(|\hat{\beta}^{(b)}| < \hat{\beta})/B$ . We summarize our Type I error results at the 0.05 significance level in Table 1 which demonstrates that as network modularity decreases ( $q$  gets larger), the hypothesis test for  $H_0$  becomes anti-conservative. This is true for both least squares as well as GEE, although least squares is more adversely impacted. In addition, while GEE excels in the highly modular setting, as expected, LS is still anti-conservative. This demonstrates the efficacy of GEE as a better inferential tool over naive least squares in network regression settings, even when GEE assumptions of between-community independence do not hold. It is also instructive to note that although the P-values for independent correlation structure are generally less than those for exchangeable structure, the differences are not overwhelming.

Table 1: **Type I error for the test of  $H_0 : \beta = 0$ .** Comparison of Type-I error at the 0.05 significance level for a network of  $n$  nodes with  $K$  balanced communities for different choices of within community edge probability ( $p$ ) and between community edge probability ( $q$ ) among GEE with independent and exchangeable correlation structure and naive least squares.

$(n, K)$	$(p, q)$	GEE (independent)	GEE (exchangeable)	LS
(200, 20)	(0.8, 0)	0.049	0.055	0.062
	(0.7, 0.1)	0.050	0.055	0.079
	(0.6, 0.2)	0.058	0.061	0.091
	(0.5, 0.3)	0.072	0.075	0.095
(400, 40)	(0.8, 0)	0.050	0.050	0.060
	(0.7, 0.1)	0.051	0.056	0.075
	(0.6, 0.2)	0.059	0.062	0.090
	(0.5, 0.3)	0.070	0.075	0.096

### 3.3 Real data analysis

Air travel networks were constructed from flight data retrieved from the Official Airline Guide (OAG), with node attribute outcomes being the country-specific COVID-19 incidence rates by month available from the Johns Hopkins University coronavirus data repository through April 30, 2020, (COVID, 19). In addition we included country-specific GDP (WBG, 2020a), total population (WBG, 2020b), and percentage of the urban population (WBG, 2020c) of the countries from the website of the World Bank as covariates. We study the effectiveness of travel bans on the incidence rate of the COVID-19 using our network regression model by performing a month-by-month analysis from January-April, 2020 which span the period of before the pandemic till one month after the travel restriction was in effect. In addition, we study the importance of baseline covariates effects such as GDP, percentage of urban population, and population size of the countries vs the network effect. The GDP and the population of the most populated countries are in the order of  $10^{12}$  and  $10^6$  respectively, so we scale these variables by  $10^{12}$ ,  $10^6$ , and  $10^2$ , respectively, in order to stabilize coefficient estimation.

With these data retrieved across different continents to model the network effect through our proposed model in (1) we assume a directed stochastic block model framework, where nodes correspond to countries and each block contains countries having a large number of commercial flights traveling among them compared to the others. Edge formation is determined by thresholding the population-normalized count of flights arriving at the destination country.

We let the incidence rate  $y_i$  of the  $i$ th country to be the number of cases per 1000 populations, and the covariates  $\mathbf{x}_{i_{n \times 4}} = (\mathbf{1}_{n \times 1} : \mathbf{x}_{i2_{n \times 1}} : \mathbf{x}_{i3_{n \times 1}} : \mathbf{x}_{i4_{n \times 1}})$  to be a matrix whose first column has 1s as the intercept and the second, third and fourth columns have the population size, GDP, percentage of the urban population of the  $i$ th country scaled by  $10^6$ ,  $10^{12}$ , and  $10^2$  respectively. For constructing the adjacency matrix  $\mathbf{A}$ , we consider two scenarios: unweighted and weighted. For unweighted adjacency matrices, from the directed

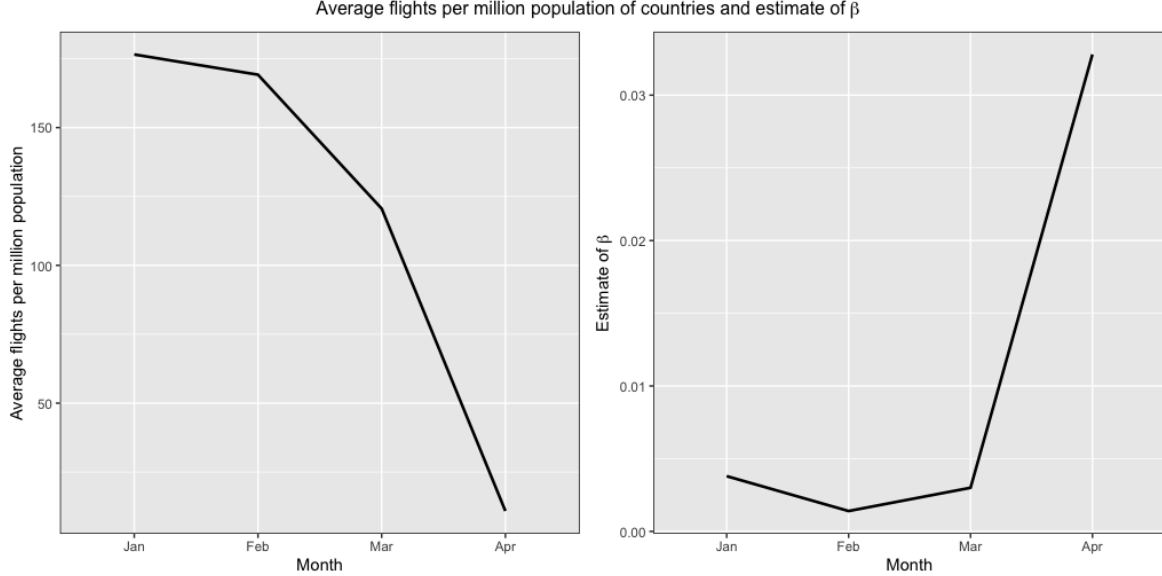


Figure 2: **Changes in air travel networks and the impact of incidence rates over time.** Monthly average number of flights per million population over the countries and monthly estimate of  $\beta$  for Jan-Apr 2020 demonstrate a downward and an upward trend, respectively.

graph dictated by the number of flights in a particular month, we first construct a count matrix  $\mathbf{C}$  that counts the number of flights from one country to the other. Then we construct an unweighted adjacency matrix  $\mathbf{A}$  with 0s and 1s where the entry of  $\mathbf{A}$  is 1 if it exceeds the third quartile of the elements of  $\mathbf{C}$ , and 0 otherwise. For weighted adjacency matrices we divide the elements of  $\mathbf{C}$  by the total population of the destination country per million. The main rationale behind this scaling is that one would expect more flights traveling to a populated country compared to a less populated country. Therefore, dividing it by the population of the country will result in the elements of the weighted adjacency matrix being on the same scale.

With the two adjacency matrices constructed in this way, we fit model (3) and summarize the results in Table 2. The estimates of  $\beta$  increase from February to April both for the weighted and unweighted cases suggesting that there is an increasing association between the travel and spread of the pandemic. To further investigate this behavior, we plot the average number of flights per million population in Figure 2 which shows that although the average

number of flights is decreasing from January to April, the estimates of  $\beta$  are increasing. This reflects the fact that while travel bans led to a decrease in the total number of flights in March and April, the increasing  $\beta$  in these months implies that each flight had an increased likelihood of transmitting COVID-19 to the destination country, increasing the correlation between the incidence rates in the two countries.

Table 2 also demonstrates that while the overall population of a country has a negligible effect on the incidence rate leading to smaller values of  $\alpha_2$ , the percentage of the urban population plays a crucial role especially when the travel ban has already been in effect, for example, the value of  $\alpha_4$  is 62 (55 for weighted case) in April compared to 0 in February. Moreover, the corresponding values are consistent for weighted and unweighted networks.

Table 2 also demonstrates the utility of including baseline covariates alongside network effect to study the effectiveness of travel bans in mitigating the spread of COVID-19. By comparing the values of  $\beta$  and  $\alpha_4$ , one can note that for the initial months of the pandemic, the network effect is more compared to the effect of urban population. However, when the travel ban has already taken place during March (for most of the countries), the effect of urban population supersedes the network effect as its value increase to 62.33 drastically from 9.88 suggesting that urbanity is the next important factor to consider for controlling the spread of the pandemic after the travel bans.

We also compare our results with naive least squares in Table 3 which shows coefficient estimates for both models. Of note, the April estimate of  $\beta$  is dramatically larger in the naive least squares model, which may be a manifestation of the increased bias we expect to see for naive least squares. Standard errors for the coefficient estimates are uniformly smaller for least squares as we expect, likely a representation of the overconfidence of the least squares model that comes from ignoring network induced correlation. This case demonstrates that using least squares would incorrectly dramatically increase both the magnitude and degree of significance of the network effects on incidence rates, particularly in the months post-lockdown when travel bans were in place. In contrast, the GEE model provides a more

realistic view.

Table 2: **Estimates of the parameters for unweighted and (weighted) networks under the GEE model.**  $\beta, \alpha_1, \alpha_2, \alpha_3$  and  $\alpha_4$  correspond to the coefficients of the adjacency matrix (network effect), intercept, population, GDP, and percentage of the urban population, respectively.

Month of 2020	$\beta$	$\alpha_1$	$\alpha_2$	$\alpha_3$	$\alpha_4$
Jan	1.8759 (0.0038)	-0.0002 (-0.0001)	0.0000 (0.0000)	0.0013 (0.0013)	0.0003 (0.0000 )
Feb	2.1946 (0.0014)	-0.0048 (-0.0037)	0.0000 (0.0000)	0.0555 (0.0575)	-0.0094 (-0.0072 )
Mar	2.7186 (0.0030)	-0.7846 (-0.7490)	-0.0005 (-0.0007)	-0.1446 (-0.0233)	9.8844 (9.8862 )
Apr	4.6574 (0.0328)	-4.7307 (-3.5655)	-0.0085 (-0.0125)	0.0626 (0.4685)	62.3300 (54.9767)

Table 3: **Comparison of the naive linear regression with GEE for the weighted networks.** The numbers reported in the parenthesis correspond to our GEE method while the others correspond to least squares.  $\beta, \alpha_1, \alpha_2, \alpha_3$  and  $\alpha_4$  correspond to the coefficients of the adjacency matrix, intercept, population, GDP, and percentage of the urban population respectively.

Month of 2020	$\beta$	$\alpha_1$	$\alpha_2$	$\alpha_3$	$\alpha_4$
Jan	0.0424 (0.0038)	-0.0001 (-0.0001)	0.0000 (0.0000)	0.0013 (0.0013)	0.0000 (0.0000 )
Feb	0.0105 (0.0014)	-0.0037 (-0.0037)	0.0000 (0.0000)	0.0576 (0.0575)	-0.0073 (-0.0072 )
Mar	0.0458 (0.0030)	-0.7060 (-0.7490)	-0.0009 (-0.0007)	0.0017 (-0.0233)	9.5519 (9.8862 )
Apr	1.2655 (0.0328)	-5.5415 (-3.5655)	-0.0073 (-0.0125)	-0.2041 (0.4685)	67.5900 (54.9767)

## 4 Discussion

We have proposed a generalized estimating equation (GEE) approach to network regression model. Assuming independent community structure and using the simultaneous estimation of memberships, the GEE approach allows for community dependent covariate coefficient estimation, and thereby provides a flexible and efficient solution to the network regression model. Moreover, this allows us to do a hypothesis testing of the network regression parameter  $\beta$  which helps us to decide the importance of including such term in our analysis. We provided a relevant real data example of COVID-19 cases along with baseline covariates such as GDP, population size, and percentage of urban population of countries across

different continents, and the number of commercial flights traveling between them to study the importance of travel bans to mitigate the spread of the COVID-19 pandemic. We have constructed the adjacency matrix from the count of flights rendered in a network of countries via a stochastic block model where each block contains countries having a similar number of flights. Our proposed model has helped us to understand the importance of the baseline covariates vs network effect. Since we have dealt with longitudinal data, it is also instructive to note that our proposed model offers us the flexibility of clustering both in the network space and also over time.

One limitation of our results is the balanced community assumption made in Proposition 3.1 which may not reflect some unbalanced networks. This assumption can be relaxed somewhat with small departures from the balanced design. Further, under the stochastic block model, extremely unbalanced networks still allow for consistent estimation of  $p$  and  $q$ , however for a more flexible network model that allows for community-specific edge probabilities, consistent estimation of edge probabilities requires each community to grow asymptotically with  $n$ .

## 5 Appendix

### 5.1 Proof of Proposition 3.1

From the construction of the adjacency matrices, one can note that the entries  $A_{ij}$ s are i.i.d. Bernoulli random variables with

$$E(A_{ij}) = \begin{cases} p, & \text{if } i, j \text{ belong to the same community} \\ q, & \text{otherwise} \end{cases}$$

and

$$Var(A_{ij}) = \begin{cases} p(1-p), & \text{if } i, j \text{ belong to the same community} \\ q(1-q), & \text{otherwise} \end{cases}$$

Denote by  $S$  the set  $\{i, j : 1 \leq i < j \leq n, i, j \text{ belongs to the same community}\}$ , and its complement by  $S'$ . Therefore, for a directed graph, one can write

$$\begin{aligned} E\left(\sum_{i,j \in S} A_{ij}\right) &= 2K \binom{m}{2} p, \\ Var\left(\sum_{i,j \in S} A_{ij}\right) &= 2K \binom{m}{2} p(1-p) = s_{m_p}^2, \\ E\left(\sum_{i,j \in S'} A_{ij}\right) &= K(K-1)m^2q, \text{ and} \\ Var\left(\sum_{i,j \in S'} A_{ij}\right) &= K(K-1)m^2q(1-q) = s_{m_q}^2. \end{aligned}$$

Next, one can verify Lindeberg condition to establish the central limit theorem:

$$\frac{\sum_{i,j \in S} A_{ij} - 2K \binom{m}{2} p}{\sqrt{2K \binom{m}{2} p(1-p)}} \quad \text{and} \quad \frac{\sum_{i,j \in S'} A_{ij} - K(K-1)m^2q}{\sqrt{K(K-1)m^2q(1-q)}} \xrightarrow{d} N(0, 1) \quad (4)$$

as  $Km^2p(1-p)$  and  $Km^2q(1-q) \rightarrow \infty$ .

The Lindeberg's condition requires us to verify

$$\frac{1}{s_{m_p}^2} \sum_{i,j \in S} E\left(B_{ij}^2 I_{\{|B_{ij}| \geq \epsilon s_{m_p}\}}\right) \rightarrow 0 \quad \text{and} \quad \frac{1}{s_{m_q}^2} \sum_{i,j \in S'} E\left(B_{ij}^2 I_{\{|B_{ij}| \geq \epsilon s_{m_q}\}}\right) \rightarrow 0,$$

where  $B_{ij} = A_{ij} - E(A_{ij})$ . Since  $|B_{ij}| \leq 1$ , the above condition is satisfied when  $Km^2p(1-p)$  and  $Km^2q(1-q)$  tend to  $\infty$  under which  $\epsilon s_{m_p}$  and  $\epsilon s_{m_q}$  are both greater than 1.

Dividing the numerator and denominator of (4) by  $2K\binom{m}{2}$  and  $K(K-1)m^2$  respectively, one obtains both

$$m^{\gamma/2} \sqrt{2K\binom{m}{2}} \frac{\sum_{i,j \in S} A_{ij} / \binom{2K\binom{m}{2}}{2} - p}{\sqrt{m^\gamma p(1-p)}} \quad \text{and} \quad m^{\gamma/2} \sqrt{K(K-1)m^2} \frac{\sum_{i,j \in S'} A_{ij} / \binom{K(K-1)m^2}{2} - q}{\sqrt{m^\gamma q(1-q)}}$$

both converge to  $N(0, 1)$  distribution. Since  $\hat{p} = \sum_{i,j \in S} A_{ij} / \binom{K\binom{m}{2}}{2}$ , and  $\hat{q} = \sum_{i,j \in S'} A_{ij} / \binom{K(K-1)m^2}{2}$ , both  $\hat{p}$  and  $\hat{q}$  are  $m^{1+\gamma/2}$  consistent.

## 5.2 Proof of Theorem 3.2

Here we present the sketch of the proof of Theorem 3.2. One can write (3) as

$$\sum_{k=1}^K U_k(\alpha, \boldsymbol{\beta}, p, q) = \sum_{k=1}^K \mathbf{D}_k^\top \mathbf{V}_k^{-1} \mathbf{S}_k = 0, \quad (5)$$

where  $\mathbf{S}_k = \mathbf{y}_k - \boldsymbol{\mu}_k$ , and  $U$  is a function of the model parameters.

Let  $\mathbf{b} = (\beta, \boldsymbol{\alpha})^\top$  denote the vector of model parameters, and  $\boldsymbol{\pi} = (p, q)^\top$  denote the vector of model parameters, and vector of within and between edge probabilities respectively. Letting  $\mathbf{b}$  fixed, the Taylor expansion yields

$$\begin{aligned} \frac{\sum_{k=1}^K U_k(\mathbf{b}, \boldsymbol{\pi}^*)}{K^{1/2}m^{1+\gamma/2}} &= \frac{\sum_{k=1}^K U_k(\mathbf{b}, \boldsymbol{\pi})}{K^{1/2}m^{1+\gamma/2}} + \frac{\sum_{k=1}^K \frac{\partial U_k(\mathbf{b}, \boldsymbol{\pi})}{\partial \boldsymbol{\pi}}}{K^{1/2}m^{1+\gamma/2}} m^{1+\gamma/2} (\boldsymbol{\pi}^* - \boldsymbol{\pi}) + o_P(1) \\ &= \tilde{A} + \tilde{B}\tilde{C} + o_P(1), \end{aligned} \quad (6)$$

One can note that  $\tilde{B} = o_P(1)$  as  $\partial U_k(\mathbf{b}, \boldsymbol{\pi}) / \partial \boldsymbol{\pi}$  are linear functions of  $\mathbf{S}_k$ 's defined in (5) whose means are zero, and  $\tilde{C} = O_P(1)$  thanks to Proposition 3.1. Therefore,  $\frac{\sum_{k=1}^K U_k(\mathbf{b}, \boldsymbol{\pi}^*)}{K^{1/2}m^{1+\gamma/2}}$  is asymptotically equivalent to  $\frac{\sum_{k=1}^K U_k(\mathbf{b}, \boldsymbol{\pi})}{K^{1/2}m^{1+\gamma/2}}$  whose asymptotic distribution is multivariate

normal with zero mean and covariance is equal to  $V$  as defined in Theorem 3.2. The proof is thus complete following Liang & Zeger (1986).

## 6 Acknowledgement

RG would like to thank Anupam Kundu, postdoctoral associate at Yale School of Public Health and Thien Le, postdoctoral fellow at Harvard for many useful discussions regarding real data processing. JP acknowledges support from R01AI138901, and IB acknowledges support from R01MH116884.

## References

Aukett, R., Ritchie, J., & Mill, K. (1988). Gender differences in friendship patterns. *Sex roles, 19*(1), 57–66.

Bank, W. (2020). *Covid-19 to plunge global economy into worst recession since World War II*. World Bank Group Washington, DC.

Binkiewicz, N., Vogelstein, J. T., & Rohe, K. (2017). Covariate-assisted spectral clustering. *Biometrika, 104*(2), 361–377.

Burton, P., Gurrin, L., & Sly, P. (1998). Extending the simple linear regression model to account for correlated responses: an introduction to generalized estimating equations and multi-level mixed modelling. *Statistics in Medicine, 17*(11), 1261–1291.

Chen, M., Kato, K., & Leng, C. (2021). Analysis of networks via the sparse  $\beta$ -model. *Journal of the Royal Statistical Society: Series B (Statistical Methodology)*.

Christakis, N. A., & Fowler, J. H. (2007). The spread of obesity in a large social network over 32 years. *New England Journal of Medicine, 357*(4), 370–379.

COVID, G. (19). database (2021) retrieved from <https://github.com/cssegisanddata/COVID-19>.

Diggle, P., Diggle, P. J., Heagerty, P., Liang, K.-Y., Zeger, S., et al. (2002). *Analysis of longitudinal data*. Oxford University Press.

Halekoh, U., Højsgaard, S., & Yan, J. (2006). The r package geepack for generalized estimating equations. *Journal of Statistical Software*, 15/2, 1–11.

Hoff, P. (2021). Additive and multiplicative effects network models. *Statistical Science*, 36(1), 34–50.

Hoff, P. D., Raftery, A. E., & Handcock, M. S. (2002). Latent space approaches to social network analysis. *Journal of the American Statistical Association*, 97(460), 1090–1098.

Holland, P. W., Laskey, K. B., & Leinhardt, S. (1983). Stochastic blockmodels: First steps. *Social Networks*, 5(2), 109–137.

Holland, P. W., & Leinhardt, S. (1981). An exponential family of probability distributions for directed graphs. *Journal of the American Statistical Association*, 76(373), 33–50.

Igarashi, T., Takai, J., & Yoshida, T. (2005). Gender differences in social network development via mobile phone text messages: A longitudinal study. *Journal of Social and Personal Relationships*, 22(5), 691–713.

Kelejian, H. H., & Prucha, I. R. (1998). A generalized spatial two-stage least squares procedure for estimating a spatial autoregressive model with autoregressive disturbances. *The Journal of Real Estate Finance and Economics*, 17(1), 99–121.

Le, T.-M., Raynal, L., Talbot, O., Hambridge, H., Drovandi, C., Mira, A., ... Onnela, J.-P. (2022). Framework for assessing and easing global covid-19 travel restrictions. *Scientific Reports*, 12(1), 1–13.

Liang, K.-Y., & Zeger, S. L. (1986). Longitudinal data analysis using generalized linear models. *Biometrika*, 73(1), 13–22.

Mandel, F., Ghosh, R. P., & Barnett, I. (2021). Neural networks for clustered and longitudinal data using mixed effects models. *Biometrics*.

Mu, C., Mele, A., Hao, L., Cape, J., Athreya, A., & Priebe, C. E. (2022). On spectral algorithms for community detection in stochastic blockmodel graphs with vertex covariates. *IEEE Transactions on Network Science and Engineering*.

Newman, M. E. (2018). Network structure from rich but noisy data. *Nature Physics*, 14(6), 542–545.

Qin, T., & Rohe, K. (2013). Regularized spectral clustering under the degree-corrected stochastic blockmodel. *Advances in Neural Information Processing Systems*, 26.

Rosvall, M., & Bergstrom, C. T. (2007). Maps of information flow reveal community structure in complex networks. *arXiv preprint physics.soc-ph/0707.0609*.

Schäfer, M., Strohmeier, M., Lenders, V., Martinovic, I., & Wilhelm, M. (2014). Bringing up opensky: A large-scale ads-b sensor network for research. In *Ipsn-14 proceedings of the 13th International Symposium on Information Processing in Sensor Networks* (pp. 83–94).

Shalizi, C. R., & Thomas, A. C. (2011). Homophily and contagion are generically confounded in observational social network studies. *Sociological Methods & Research*, 40(2), 211–239.

Shrum, W., Cheek Jr, N. H., & MacD, S. (1988). Friendship in school: Gender and racial homophily. *Sociology of Education*, 227–239.

Staber, U. (1993). Friends, acquaintances, strangers: Gender differences in the structure of entrepreneurial networks. *Journal of Small Business & Entrepreneurship*, 11(1), 73–82.

Strohmeier, M., Olive, X., Lübbe, J., Schäfer, M., & Lenders, V. (2021). Crowdsourced air traffic data from the opensky network 2019–2020. *Earth System Science Data*, 13(2), 357–366.

Tifferet, S. (2019). Gender differences in privacy tendencies on social network sites: A meta-analysis. *Computers in Human Behavior*, 93, 1–12.

VanderWeele, T. J. (2011). Sensitivity analysis for contagion effects in social networks. *Sociological Methods & Research*, 40(2), 240–255.

WBG. (2020a). Available online: <https://data.worldbank.org/indicator/ny.gdp.mktp.cd>. *CD (accessed on 2 September 2022)*.

WBG. (2020b). Available online: <https://data.worldbank.org/indicator/sp.pop.totl>. *CD (accessed on 2 September 2022)*.

WBG. (2020c). Available online: <https://data.worldbank.org/indicator/sp.urb.totl.in.zs>. *CD (accessed on 2 September 2022)*.

Zeger, S. (1986). The analysis of discrete and continuous longitudinal data. *Biometrics*, 42, 121–130.